Characterization of local electrochemical doping of high performance conjugated polymer for photovoltaics using scanning droplet cell microscopy[☆]

Jacek Gasiorowski[a], Andrei Ionut Mardare[b], Niyazi Serdar Sariciftci[a], Achim Walter Hassel[b,*]

[a] Linz Institute for Organic Solar Cells (LIOS), Physical Chemistry, Austria
[b] Institute for Chemical Technology of Inorganic Materials, Johannes Kepler University, Linz, Austria

ABSTRACT

The electrochemical oxidation of a next generation low bandgap high performance photovoltaic material namely poly[4,8-bis-substituted-benzo[1,2-b:4,5-b0]dithiophene-2,6-diyl-alt-4-substituted-thieno[3,4-b] thiophene-2,6-diyl] (PBDTTT-c) thin film was investigated using a scanning droplet cell microscope. Cyclic voltammetry was used for the basic characterization of the oxidation/doping of PBDTTT-c. Application of the different final potentials during the electrochemical study provides a close look to the oxidation kinetics. The electrical properties of both doped and undoped PBDTTT-c were analyzed in situ by electrochemical impedance spectroscopy giving the possibility to correlate the changes in the doping level with the subsequent changes in the resistance and capacitance. As a result one oxidation peak was found during the cyclic voltammetry and in potentiostatic measurements. From Mott–Schottky analysis a donor concentration of 2.3×10^{20} cm^{-3} and a flat band potential of 1.00 V vs. SHE were found. The oxidation process resulted in an increase of the conductivity by two orders of magnitude reaching a maximum for the oxidized form of 1.4 S cm^{-1}.

1. Introduction

Organic semiconductors were developed in recent years especially due to their possible applications as cheap and environmentally friendly materials for organic electronics. Since their morphological [1] and photophysical [2] properties can be easily modified, a great effort is made for the synthesis and characterization of new organic materials, small molecules [3] and polymers [4]. Also their mechanical flexibility is a big advantage [5]. New low-band gap materials with broad absorption spectrum ranging from ultraviolet to near infrared, followed by good electrical properties were enhancing the efficiency of the organic solar cells [6,7]. From many new polymers, poly[4,8-bis-substituted-benzo[1,2-b:4,5-b0]dithiophene-2,6-diyl-alt-4-substituted-thieno[3,4-b] thiophene-2,6-diyl] (PBDTTT-c) is one of the first synthesized as a promising example of a new generation of organic semiconductor (Fig. 1). Due to its high absorption in the visible range and air stability this polymer was successfully used as a donor material in organic solar cells reaching nearly 7% efficiency [8,9]. Although much effort was put in characterization of the optical and morphological properties of this polymer and its application in the organic photovoltaics, no studies on electrochemistry and conductivity of this polymer were presented up to now.

The scanning droplet cell microscope, firstly used more than 15 years ago for localized anodic oxidation on valve metals [10] was continuously developed over time. A small electrolyte droplet coming in direct contact with the surface of the working electrode defines the investigated area, which can easily be in the μm^2 region, offering a very localized area for study. Recent works have proven its capabilities for being used in comprehensive electrochemical investigations with high reproducibility of the wetted area [11]. A complete automation of the system allows scanning over large areas while mapping various surface properties. The electrolyte confinement combined with the scanning capabilities was recently used for analysis of thin film combinatorial libraries [12,13], grain boundary electrochemistry [14] or electrochemical lithography [15,16].

---

* Corresponding author at: Altenberger Strasse 69, 4040 Linz, Austria.
Tel.: +43 732 2468 8700; fax: +43 732 2468 8905.
E-mail addresses: hassel@elchem.de, achimwalter.hassel@jku.at (A.W. Hassel).
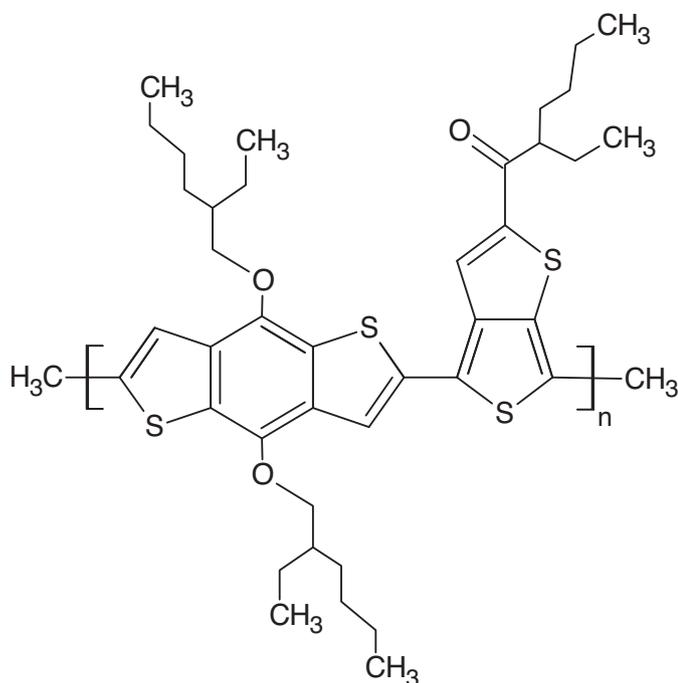
Fig. 1. Chemical structure of poly[4,8-bis-substituted-benzo[1,2-b:4,5-b0]dithiophene-2,6-diyl-alt-4-substituted-thieno[3,4-b] thiophene-2,6-diyl] (PBDTTT-c) polymer.

In the present work, a detailed electrochemical study of the PBDTTT-c was done using a scanning droplet cell microscope.

2. Experimental

A soluble poly[4,8-bis-substituted-benzo[1,2-b:4,5-b′]dithiophene-2,6-diyl-alt-4-substituted-thieno[3,4-b] thiophene-2,6-diyl] (Solarmer Co.) was used as received. The polymer structure containing benzo(1,2-b:4,5-b′)dithiophene (BDT) group co-polymerized with thieno[3,4-b]thiophene is presented in Fig. 1. The polymer was dissolved in chlorobenzene (99+%, Acros Organics) for obtaining a desired concentration of $10\,g\,L^{-1}$. The PBDTTT-c was deposited by spin coating (Solarmer Co.) on $15 \times 15\,mm^2$ glass/ITO ($15\,\Omega/\square$, Kintec Co.). Before coating, the glass substrate was cleaned by sequential sonication in acetone, isopropanol and de-ionized water. The thickness of the PDBTTT-c layer was approximately 100 nm as measured by atomic force microscopy working in tapping mode (Digital Instruments Dimension 3100, Veeco Metrology group). For all electrochemical studies, a 0.1 M solution of tetrabutylammonium hexafluorophosphate (TBAPF$_6$, ≥99%, Fluka Analytical), in propylene carbonate (PC, 99.7%, Sigma–Aldrich), was used.

Scanning droplet cell microscopy (SDCM) with a 3 electrode configuration was used for all the electrochemical investigations. Details about the construction of the SDCM and technical particularities can be found elsewhere [11,13,17]. As working electrode, glass/ITO covered with the thin layer of PBDTTT-c was used. A gold stripe helicoidally shaped (Wieland Dentaltechnik 99.999%) (2 mm wide) to prevent short-cutting with the quasi-reference electrode was used as counter electrode (CE). Since electrochemical studies were performed in a non-aqueous solution, a capillary-based reference electrode filled with agar for mechanical stability and leaking prevention, as commonly used for the SDCM, could not be used. An Ag/AgCl quasireference electrode (QRE) positioned inside the coiled CE was used instead. The QRE was prepared by electrodeposition of AgCl in 1 M HCl on an Ag wire 0.5 mm in diameter using the recipe
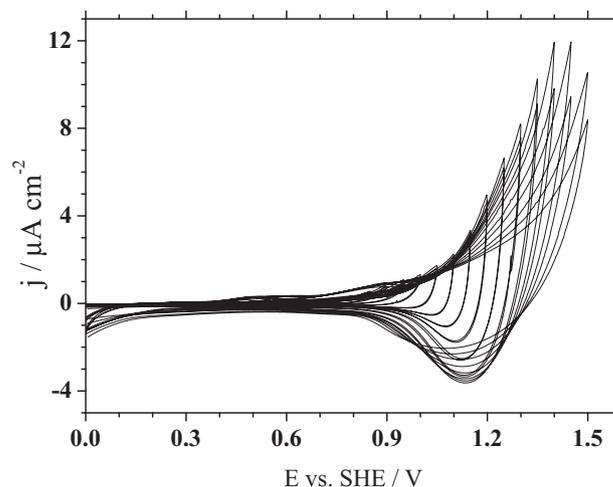

Fig. 2. Cyclic voltammetry as a function of the maximum achievable potential measured during oxidation of PBDTTT-c polymer.

presented elsewhere [18]. The potential of the QRE was found to be 0.211 V vs. SHE. According to this, all the potential values presented in this paper are referred to the SHE. Additionally, a silicone gasket at the rim of the SDCM tip was formed for allowing working with non-aqueous solutions by preventing the air contamination of the electrolyte and for ensuring a reproducible wetted area leading to a high reproducibility of the results. Since only a small electrolyte droplet comes in direct contact with the working electrode surface, even on small samples a high number of investigations can easily be done applying various electrochemical techniques or series of measurements.

For all electrochemical measurements a Solartron 1287 potentiostat in combination with a Solartron 1260 frequency response analyzer were used. Basic characterizations of the oxidation processes of PBDTTT-c were done using the cyclic voltammetry technique. For this purpose, the maximum achievable potential during oxidation was increased from 0 V vs. SHE in steps of 0.05 V up to 1.50 V vs. SHE. Different rates of the potential increase were used ranging from $1\,mV\,s^{-1}$ to $100\,mV\,s^{-1}$. The oxidation kinetics as well as the reaction reproducibility was studied additionally in the potentiostatic experiments for potentials ranging from 0 V to 1.50 V vs. SHE during oxidation. Electrochemical impedance spectroscopy (EIS) was used for characterization of the electrical properties of the PBDTTT-c film. After each potentiostatic step, EIS was additionally done for measuring the impedance of the system, For this purpose, a peak-to-peak AC perturbation of 0.02 V was applied and the frequency was scanned from 100 kHz to 1 Hz with the bias previously used in the potentiostatic experiments. Additionally, the doping level in PBDTTT-c polymer during the oxidation process was characterized using Mott–Schottky analysis in the potential range of 0–1.50 V vs. SHE.

3. Results and discussion

3.1. Cyclic voltammetry characterization

The electrochemical oxidation of PBDTTT-c was studied in a series of cyclic voltammograms measured with increased achievable final potential and the results are presented in Fig. 2. During the experiment, the maximum potential was increased from 0 V vs. SHE in steps of 0.05 V up to 1.50 V vs. SHE in order to probe the effect of doping of the polymer. For each measurement, two consecutive cycles were performed for probing the reproducibility of the oxidation process. As it can be observed, above 0.95 V vs. SHE an

increase in the current, due to the beginning of the electrochemical oxidation process, was detected. This increase is fully reversible and is followed by a reduction process. The minimum of this reduction process is found at 1.15 V vs. SHE. Since the polymer was developed to serve as a donor in organic photovoltaic devices, the reversibility of the electrochemical oxidation process suggests a possible hole transporting property of this material. Further increasing the potential above 0.95 V vs. SHE, an almost linear increase in the maximum measured current is noticeable up to 1.4 V vs. SHE. Above this potential, a sudden decrease of the maximum current achieved due to the degradation process is observed. This process is related to the dissolution of the oxidized PBDTTT-c layer in PC as well as to a possible incipient degradation of the electrolyte or substrate. Additionally, above 1.3 V vs. SHE a strong difference between the first and the second scan is found. This difference increases with the increase in the applied potential. This behaviour, suggesting an irreversibility of the oxidation process, may be due to the degradation of the PBDTTT-c which starts to be dominant at high potentials. At the same time, the reduction process changes due to the same reason. A decrease in the peak minimum followed by a broadening of this peak is noticeable. This can be attributed to a degradation of the polymer layer. Interestingly, for this type of polymer no distinct oxidation peak was observed, but rather a continuous current increase until the maximum potential is reached.

3.2. Potentiostatic characterization

For a better understanding of the electrochemical doping, time dependent potentiostatic experiments with different maximum achieved potentials were performed. The potential was increased step-wise from 0.0 V vs. SHE up to 1.5 V vs. SHE in 0.05 V steps for a precise determination of the oxidation potential. For the entire measurement series, the layer of PBDTTT-c was kept for 10 s at the corresponding constant potential and the transient current response was measured. A data acquisition rate of 10 Hz corresponding to a time resolution of 100 ms was used. The changes of the current in the transients as a function of the applied potential during the electrochemical oxidation process of PBDTTT-c are presented in Fig. 3a as a 3D plot. For potentials below 1.0 V vs. SHE only background currents in the range of $10^{-8} - 10^{-7}$ A cm^{-2} can be observed. Above this potential, the first values of the recorded current transients are much higher than the background level. These values increase according to the increase of the potential driving the oxidation process. The highest transient current measured after the first 100 ms was found at 1.3 V vs. SHE. Above this potential, a strong decrease of these first values is noticeable. This may be correlated with the results obtained from the cyclic voltammograms presented in Fig. 2. Starting from a potential of approximately 1.3 V vs. SHE, the maximum achievable current at the end of each CV sweep was decreasing. Additionally, the shift between the two subsequently recorded sweeps for each measurement was the highest. Combined with the results obtained from the potentiostatic experiments, this suggests that above 1.30 V vs. SHE a degradation process of the polymer film starts.

In order to better describe the electrochemical oxidation of PBDTTT-c, the current densities at the end of the potentiostatic experiments (after 10 s of applying the constant potential) are presented in Fig. 3b as a function of the potential. As it can be noticed, up to 1.0 V vs. SHE only a small increase of the current densities can be measured. These values are describing the background current flowing through the electrochemical cell. Starting from 1.0 V vs. SHE a continuous increase in the value of the current density
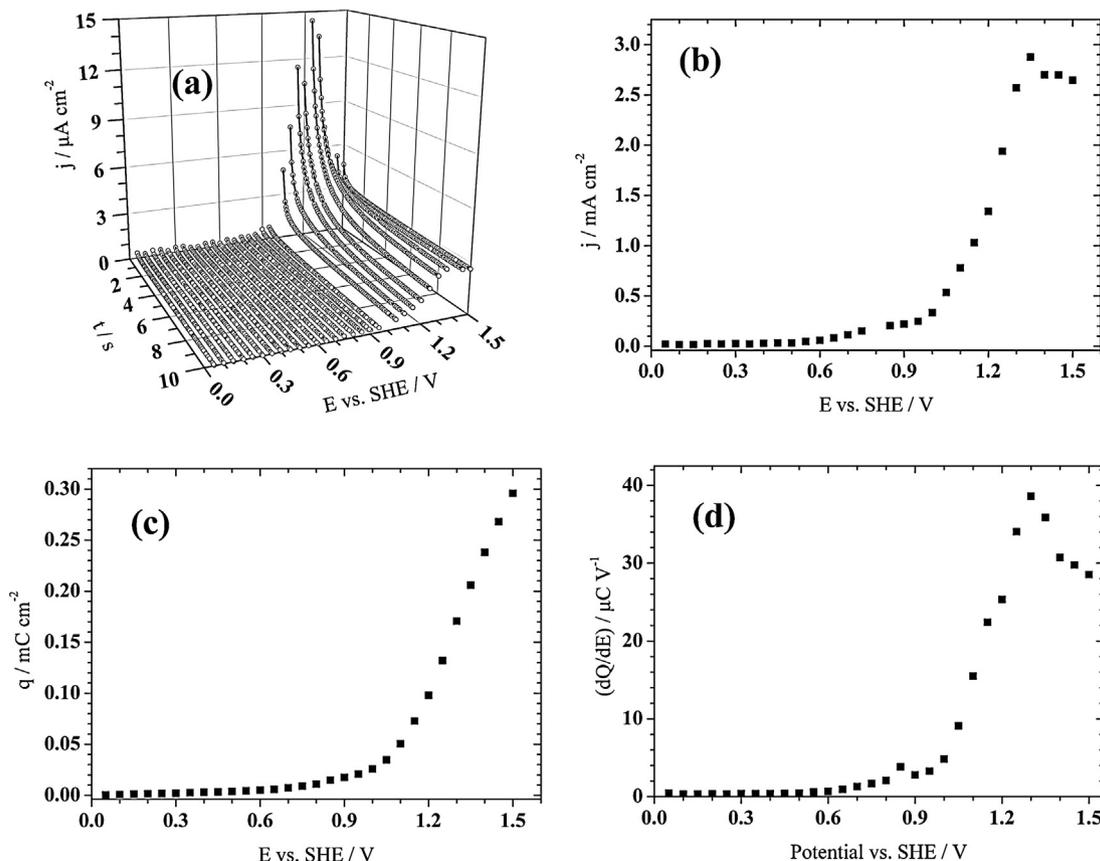

Fig. 3. Time dependent potentiostatic characterization during oxidation of PBDTTT-c (a). Analysis of potentiostatic measurement during oxidation process. The current density (b), charge density (c) and charge variation (d) are plotted as a function of applied potential.

can be observed. This may be attributed to a continuous increase in the PBDTTT-c conductivity due to the oxidation process which will have as a result an increase in the background current, as previously also observed in Fig. 3a. Above 1.3 V vs. SHE, a small decrease in the current density can be observed at the end of the potentiostatic experiments. The same trend was previously found in the cyclic voltammograms from Fig. 2 and together may be attributed to a potential driven degradation process in the PBDTTT-c.

The integration of the individual potentiostatic transients gives information about the charge consumed at each potential step during the electrochemical oxidation process. The total charge can then be calculated by summation of all individually measured charges consumed at each potentiostatic step. The total charge dependence on the maximum applied potential is plotted in Fig. 3c. Similarly to the current density behaviour, only a small change in the total charge taking part in the electrochemical transfer can be found for potentials up to 1.0 V vs. SHE. However, above 1.0 V vs. SHE a strong increase of the total charge is observed. This is related to the electrochemical oxidation process in the PBDTTT-c. Additionally, a linear behaviour was found for the charge density dependence on the applied potential above 1.0 V vs. SHE. No charge saturation is observed in this plot. This fact is similar to the previously analyzed behaviour during the cyclic voltammetry (Fig. 2). The intercept of the linear fit presented in Fig. 3c shows a value of 1.05 V vs. SHE which can be considered the starting potential of the oxidation process.

The amount of charge consumed in the electrochemical process for each equidistant applied potential can be directly probed by plotting dQ/dE as a function of the potential. Since the charge value is calculated for each potential step after equilibrium is attained, this plot will describe the infinitesimal changes in the electrochemical system. The results are presented in Fig. 3d. The plot reveals that for potentials below 1.0 V vs. SHE no significant changes occur, suggesting an oxidation of the PBDTTT-c at higher potentials. Above 1.0 V vs. SHE an increase in the charge consumed by the electrochemical system at each potential step was found describing one more time the oxidation process of the polymer. A peak with maximum at 1.3 V vs. SHE could be identified marking the beginning of the potential range where the polymer degradation starts. By polymer degradation one should understand the dissolution of the oxidized form in the electrolyte.

3.3. Electrochemical impedance spectroscopy

The electrical properties during electrochemical doping of the PBDTTT-c were investigated using electrochemical impedance spectroscopy. During this study, the changes of the resistance and capacitance of the oxidized polymer can be detected. In the present study all the measurements were done just after each potentiostatic experiment which was previously discussed in Fig. 3. Every potentiostatic pulse of 10 s duration, necessary for establishing an equilibrium state of the electrochemical process at a given potential, was followed by an impedance measurement in a broad frequency range. For each impedance step, a bias equal to the constant potential previously used in the potentiostatic experiment was applied. Between switching from the potentiostatic measurements to the impedance, the electrochemical cell was always under constant potential control referenced to the SHE. During the entire EIS, the SDCM addressed a single measurement spot and the frequency response analyzer recorded the real and imaginary parts of the impedance. Further, the impedance modulus and the phase shift are calculated by transforming the Cartesian coordinate system into a polar coordinate system according to the Bode representation. The Bode plots of the impedance spectroscopy on PBDTTT-c are presented in Fig. 4. In the part (a) of Fig. 4 the impedance is plotted as a function of the frequency for the entire analyzed spectrum. All measurements obtained at different biases immediately after the potentiostatic treatment are presented together. The arrow indicates the direction of the potential increase. At low biases up to 0.9 V vs. SHE, only a small change in the impedance can be observed. Above this threshold the impedance starts to decrease due to the progressive oxidation of the PBDTTT-c layer. Eventually, at applied biases as high as 1.3 V vs. SHE, the impedance value reaches a minimum limited by the electrolyte resistance of approximately 20 kΩ which can be directly observed at high frequency. The part (b) of Fig. 4 shows the associated phase shift measured during the electrochemical impedance spectroscopy. Similar to the previous case, the arrow describes the direction of the potential increase. At low biases, the phase shift has an invariant behaviour up to 0.90 V vs. SHE, which is consistent with the data obtained from the impedance spectra. A capacitive behaviour can be identified due to the phase shifting towards negative values. Above this potential, the phase shift starts to increase during the oxidation process of PBDTTT-c suggesting a progressive increase in the layer conductivity due to the doping effect. For organic materials, this can be attributed to an insulator/metal transition which in the present case will weaken the dominant capacitive behaviour [18]. The shapes of the phase shifts suggest a two-time constant equivalent circuit, which is best observed in the potential range corresponding to the oxidation process. The equivalent circuit describing the electrochemical system used is presented
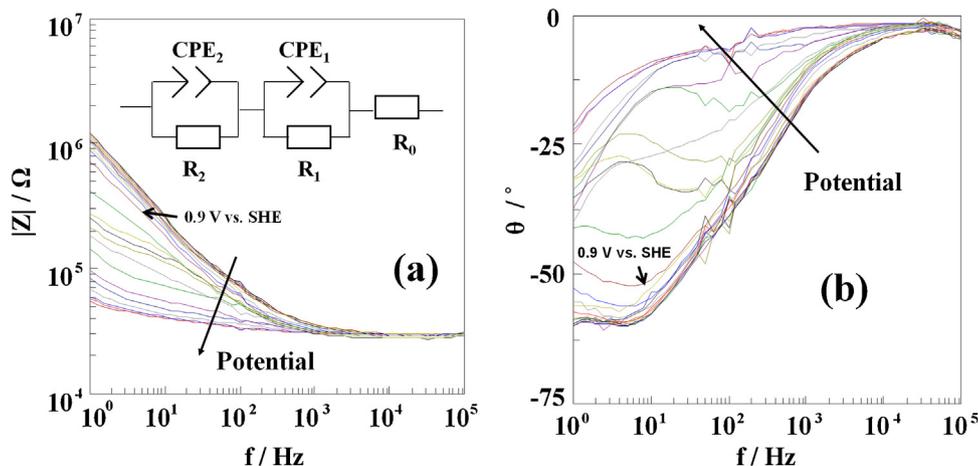

Fig. 4. Bode plots of impedance (a) and phase (b) as a function of frequency measured in Mott-Schottky regime during electrochemical oxidation. The measurement where done between 0 and 1.5 V vs. SHE.
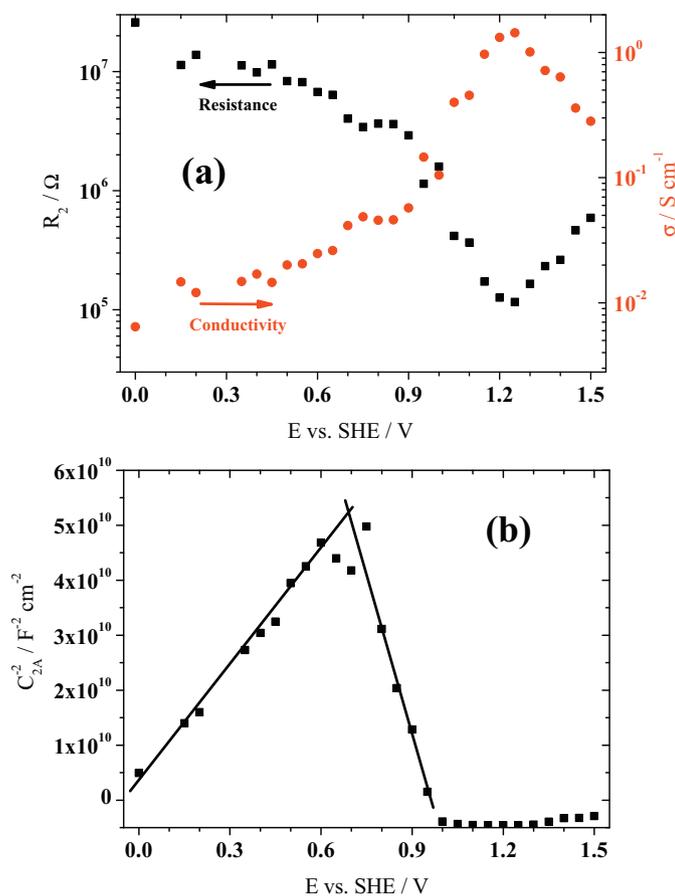
Fig. 5. Resolved electrical parameters from EIS study: (a) resistance values of PBDTTT-c layer plotted together with corresponding conductivity values and (b) Mott-Schottky plot of the conductivity.

as an inlet in Fig. 4a. Two constant phase elements (CPE) in parallel with resistances are connected in series with the electrolyte resistance (R_0). The two RC elements (1 and 2) are describing the electrolyte/polymer interface and the PBDTTT-c layer, respectively.

Using the previously defined equivalent circuit, the full impedance spectra were fitted using ZView software (Scribner Associated) in order to obtain the electrical properties of the undoped and electrochemically doped PBDTTT-c layer. The constant phase elements fit had errors of maximum 3% for the capacitances. The CPE$_1$ describing the PBDTTT-c layer showed an exponent of minimum 0.85 suggesting a behaviour consistent to that of a real capacitor. The impedance measurements done at various applied biases define a Mott–Schottky type of analysis usually involved in the semiconductor properties studies. In Fig. 5a these results are summarized. At low biases up to 0.90 V vs. SHE only a small changing in the film resistance can be observed. These values obtained from electrochemical impedance spectroscopy are in the range of tens of MΩ. The changes in the film resistance can be related to a slow doping of the polymer in contact with the electrolyte. This effect was observed in the previously described cyclic voltammetry and potentiostatic measurements as a background current. Above this potential a strong decrease of the polymer resistance down to approximately 100 kΩ can be measured. This is due to the electrochemical oxidation of the PBDTTT-c. The process of the layer oxidation is dominant for potentials up to 1.25 V vs. SHE, above which an increase in the resistance can be noticed. Similar to the case of cyclic voltammetry and potentiostatic measurements, this growth of the resistance value can be attributed to the degradation (dissolution) of the PBDTTT-c layer. Since the

material was developed to work as a conducting polymer in organic electronics, in addition to the resistance values, the conductivity values (σ) measured during the electrochemical process are given. The results are presented in the Fig. 5a. For low applied potentials, the large measured film resistance is equivalent to the low film conductivity in the range of mS cm^{-1}. Since the conductivity of the undoped polymer should be in the range of μS cm^{-1}, this conductivity value is surprisingly high [19]. However, this could be explained by considering that a certain doping takes place through spontaneous ion diffusion due to the direct contact between polymer and electrolyte. After initiation of the oxidation process at 0.90 V vs. SHE, a strong increase in conductivity is found up to 1.25 V vs. SHE. In this region, the value of conductivity increases by two orders of magnitude reaching a maximum of 1.4 S cm^{-1}. Considering the high photovoltaic performance achieved in a solar cell containing PBDTTT-c, this relatively low value of the conductivity measured after doping is surprising when compared to other conducting polymers such as P3HT [20]. For biases higher than 1.25 V vs. SHE, a decrease in the conductivity is observed according to the dissolution of the PBDTTT-c.

The semiconducting properties of PBDTTT-c were characterized using Mott-Schottky analysis conducted during the performance of the electrochemical impedance spectroscopic study. According to the theory [21,22] the capacitance values determined from CPE$_2$ measured during the impedance spectroscopy were first normalized to the investigated area. Furthermore, the obtained normalized capacitance was inverse squared and the resulting values are presented in Fig. 5b as a function of the applied potential. For bias values of up to 0.75 V vs. SHE, the value of the inversed square capacitance increases. This behaviour can be attributed to the formation of an inversion layer leading to an apparent n-type conductivity. Between 0.75 and 1.00 V vs. SHE a slope describing the semiconducting properties of the PBDTTT-c due to the electrochemical oxidation can be observed. In this region, the PBDTTT-c layer has still a very low conductivity and the polymer can still be described as a semiconductor. Using the Mott–Schottky formulation:

$$C_{2A}^{-2} = \frac{2(E - E_{fb} - kT/e)}{e\varepsilon\varepsilon_0 N_D} \tag{1}$$

the donor density and the flat band potential were calculated. In Eq. (1) C_{2A}^{-2} is the area normalized inverse square capacitance, e is the elementary charge, ε is the relative PBDTTT-c permittivity (in this study considered 3.5), ε_0 is the vacuum permittivity, E is the applied potential and E_{fb} is the flat band potential. For biases below 0.60 V, were the inversion layer describing the n-type conductivity can be found, an electron concentration of 5.6×10^{20} cm^{-3} was calculated using a linear fitting of the experimental points presented in Fig. 5b. In this case a flat band potential of -0.10 V vs. SHE was calculated. For the p-type conduction region above 0.75 V vs. SHE, a donor concentration of 2.3×10^{20} cm^{-3} was found. Additionally, a flat band potential of 0.95 V vs. SHE was calculated taking into account the thermal contribution from kT/e of 25.8 mV. For biases above 1.00 V vs. SHE an electrochemically doped PBDTTT-c cannot be considered anymore as a semiconductor but rather as a metal.

4. Conclusions

Scanning droplet cell microscopy was used for localized electrochemical investigations of a PBDTTT-c thin film. The electrochemical oxidation of this new low band gap polymer was studied by cyclic voltammetry. No distinct oxidation peak was observed, but rather a continuous current increase until the maximum applied potential is reached. This result was confirmed by potentiostatic measurements. From the current transients and the calculated charge consumed in the electrochemical process

as function of applied potential, the existence of an oxidation peak with a maximum at 1.30 V vs. SHE was confirmed. The electrical characterization of the polymer was performed by electrochemical impedance spectroscopic measurements. The results were fitted using a simple two time constant equivalent model describing the behaviour of the polymer layer during electrochemical process. As expected during the doping process, an increase in the electrical conductivity was determined showing the insulator/semiconductor/metal transitions. For characterization of the doping level in the semiconducting state, an additional Mott–Schottky analysis was applied and a hole conduction mechanism was evidenced.

Acknowledgements

References

[1] H. Hoppe, N.S. Sariciftci, Organic solar cells: an overview, Journal of Materials Research 19 (2004) 1924.
[2] S.H. Park, A. Roy, S. Beaupré, S. Cho, N. Coates, J.S. Moon, D. Moses, M. Leclerc, K. Lee, A.J. Heeger, Bulk heterojunction solar cells with internal quantum efficiency approaching 100%, Nature Photonics 3 (2009) 297.
[3] M. Irimia-Vladu, E.D. Głowacki, P.A. Troshin, G. Schwabegger, L. Leonat, D.K. Susarova, O. Krystal, M. Ullah, Y. Kanbur, M.A. Bodea, V.F. Razumov, H. Sitter, S. Bauer, N.S. Sariciftci, Indigo – a natural pigment for high performance ambipolar organic field effect transistors and circuits, Advanced Materials 24 (2012) 375.
[4] E. Wang, L. Hou, Z. Wang, S. Hellstroem, F. Zhang, O. Inganaes, M.R. Andersson, An easily synthesized blue polymer for high-performance polymer solar cells, Advanced Materials 22 (2010) 5240.
[5] M. Kaltenbrunner, M.S. White, E.D. Głowacki, T. Sekitani, T. Someya, N.S. Sariciftci, S. Bauer, Ultrathin and lightweight organic solar cells with high flexibility, Nature Communications 3 (2012) 770.
[6] R. Service, Outlook brightens for plastic solar cells, Science 332 (6027) (2011) 293.
[7] M.A. Green, K. Emery, Y. Hishikawa, W. Warta, E.D. Dunlop, Solar cells efficiency tables (version 39), Progress in Photovoltaics: Research and Applications 20 (2012) 12.
[8] J. Hou, H.Y. Chen, S. Zhang, R.I. Chen, Y. Yang, Y. Wu, G. Li, Synthesis of a low band gap polymer and its application in highly efficient polymer solar cells, Journal of the American Chemical Society 131 (2009) 15586.
[9] H.-Y. Chen, J. Hou, S. Zhang, Y. Liang, G. Yang, Y. Yang, L. Yu, Y. Wu, G. Li, Polymer solar cells with enhanced open-circuit voltage and efficiency, Nature Photonics 3 (2009) 649.
[10] A.W. Hassel, M.M. Lohrengel, Preparation and properties of ultra thin anodic valve metal oxide films, Materials Science Forum 185 (1995) 581.
[11] A.I. Mardare, A.W. Hassel, Quantitative optical recognition of highly reproducible ultrathin oxide films in microelectrochemical anodization, Review of Scientific Instruments 80 (2009), 046106-3.
[12] A.I. Mardare, A.P. Yadav, A.D. Wieck, M. Stratmann, A.W. Hassel, Combinatorial electrochemistry on Al–Fe alloys, Science and Technology of Advanced Materials 9 (2008) 035009.
[13] A.I. Mardare, A. Ludwig, A. Savan, A.D. Wieck, A.W. Hassel, Combinatorial investigation of Hf-Ta thin films ad their anodic oxides, Electrochimica Acta 55 (2010) 7884.
[14] M.T. Woldemedhin, D. Raabe, A.W. Hassel, Grain boundary electrochemistry of β-type Nb–Ti alloy using a scanning droplet cell, Physica Status Solidi A 208 (2011) 1246.
[15] A.I. Mardare, A.D. Wieck, A.W. Hassel, Microelectrochemical lithography: a method for direct writing of surface oxides, Electrochimica Acta 52 (2007) 7865.
[16] A.I. Mardare, M. Kaltenbrunner, N.S. Sariciftci, S. Bauer, A.W. Hassel, Ultra-thin anodic alumina capacitor films for plastic electronics, Physica Status Solidi A 209 (2012) 813.
[17] A.W. Hassel, M.M. Lohrengel, The scanning droplet cell and its application to structured nanometer oxide films on aluminium, Electrochimica Acta 42 (1997) 3327.
[18] A.W. Hassel, K. Fushimi, M. Seo, An agar-based silver/silver chloride reference electrode for use in microelectrochemistry, Electrochemistry Communications 1 (1999) 180.
[19] A.J. Heeger, N.S. Sariciftci, E.B. Namdas, Semiconducting and metallic polymers, 978-0-19-852864-7, Oxford University Press, 2010.
[20] R.D. McCullough, R.D. Lowe, Enhanced electrical conductivity in regioselectively synthesized poly(3-alkylthiophenes), Journal of the Chemical Society, Chemical Communications 1 (1992) 70.
[21] N.F. Mott, The theory of crystal rectifiers, Proceedings of the Royal Society London A 171 (1939) 27.
[22] W. Schottky, Zur Halbleitertheorie der Sperrschicht- und Spitzengleichrichter, Zeitschrift für Physik 113 (1939) 367.